Available online at www.sciencedirect.com
SCIENCE DIRECT
Journal of Sound and Vibration 296 (2006) 830–844
JOURNAL OF SOUND AND VIBRATION
www.elsevier.com/locate/jsvi

Dynamic stability of periodic shells with moving loads

M. Ruzzene[a], A. Baz[b,*]

[a]School of Aerospace Engineering, Georgia Institute of Technology, Atlanta, GA 30332, USA
[b]Mechanical Engineering Department, University of Maryland, College Park, MD 20742, USA

Received 28 July 2005; received in revised form 6 March 2006; accepted 8 March 2006
Available online 11 May 2006

Abstract

A moving load causes the radial displacements of an axi-symmetric shell to be several times higher than that produced by the static application of the same load. The travel velocity of the moving load affects the amplitude of the radial response and a critical velocity above which the shell response becomes unstable can be identified.

A finite element model (FEM) is developed to analyze the dynamic response of axi-symmetric shells subjected to axially moving loads. The model accounts for the effect of periodically placing stiffening rings along the shell, on the dynamic response and stability characteristics of the shell. Shape functions obtained from the steady-state solution of the equation of motion for a uniform shell are utilized in the development of the FEM. The model is formulated in a reference frame moving with the load in order to enable study of the shell stability using wave propagation and attenuation criteria. Hence, the critical velocity can be identified as the minimum velocity allowing the propagation of applied perturbations. Such stability boundaries are conveniently identified through a transfer matrix formulation.

The model is used to determine the critical velocities of the moving load for various arrangements and geometry of the stiffening rings. The obtained results indicate that stiffening the shell generally increases the critical velocity and generates a pattern of alternating stable and unstable regions.

The presented analysis provides a viable means for designing a wide variety of stable dynamic systems operating with fast moving loads such as crane booms, robotic arms and gun barrels.

1. Introduction

The analysis of moving loads on elastic structures has drawn the attention of many researchers over the last century. The extent of the efforts dedicated to studying this problem is justified by the wide variety of structures which are subjected to moving loads, such as bridges, gun barrels, rails, work pieces during machining operations as well as fluid-conveying pipes. In all these structures, the emphasis is placed on studying two basic phenomena. The first phenomenon deals with the amplification of the dynamic deflections caused by the moving loads, as compared with the deflections resulting from the static application of the same loads. The second considered phenomenon is associated with the dynamic instabilities that can be generated when the velocity of the moving loads exceeds certain critical values.

*Corresponding author. Tel.: +1 301 405 5216; fax: +1 301 405 8331.
E-mail address: baz@eng.umd.edu (A. Baz).

0022-460X/$ - see front matter © 2006 Elsevier Ltd. All rights reserved.
doi:10.1016/j.jsv.2006.03.008

Extensive efforts have been dedicated to studying the first phenomenon in order to determine the dynamic response of structures subjected to moving loads. An excellent account of the general problem of the interaction between an elastic structure and a moving load is given by Fryba [1]. The response of a beam with general boundary conditions is determined by Abu-Hilal and Mohsen in Ref. [2], where closed-form solutions are found for different types of motion of the load. Lin and Trethewey [3] investigated the dynamic response of elastic beams subjected to loads produced by moving spring–mass systems. Their finite element formulation allows for overcoming the limitations of closed-form solutions and for handling various end conditions, intermediate supports and moving loads of generally varying amplitude.

Several techniques have also been considered to analyze the second phenomenon in order to define the stability limits for various structures. Nelson and Conover [4], for example, have applied Floquet's Theory to analyze the stability of simply supported beams loaded by moving masses. The critical velocity for a Timoshenko beam on elastic foundation is investigated by Steele [5,6], through a Fourier integral solution. One of the most popular techniques involves the application of the Mathieu-Hill method, as described by Bolotin [7]. This method has also been utilized, by Benedetti [8] and Katz et al. [9], to extend the results of Nelson and Conover. For uniform and simply supported beams, Benedetti determined their stability charts, and Katz et al. investigated the stability under deflection-dependent moving loads. The application Mathieu-Hill equation is however limited to uniform and simply supported beams. In 1954, Kenney [10] investigated the stability of the steady-state response of a beam on elastic foundation by formulating the beam's equation of motion with respect to a reference coordinate system moving with the load. This approach allows for the critical velocity to be identified as the minimum velocity at which waves are free to propagate along the moving coordinate. Such a condition suggests that the analysis of the stability of the response may be considered using wave propagation and attenuation criteria. This approach is adopted by Finlayson [11] to evaluate the response of a gun barrel subjected to an expanding pressure step. In the present work, the wave propagation approach is applied to studying the stability of the steady-state response of axi-symmetric shells with stiffeners that are periodically spaced along the shell. This work is an extension of the work of Aldraihem and Baz [12] who analyzed the dynamic stability of periodic beams under moving loads using the impulsive parametric excitation theory [13,14]. Here, a finite element model (FEM) is formulated to extend the approach presented in Refs. [10,11] to shells with periodic stiffeners. The FEM is formulated in the moving coordinate system and is used to obtain the transfer matrix of a stiffened shell element. The dynamics of wave propagation in the considered class of shells are evaluated by analyzing the eigenvalues of the transfer matrix for different load velocities. The effect of stiffener's spacing and geometry, on the shell stability, is assessed through a series of numerical simulations.

The paper is organized in five sections. In the first section, a brief introduction is given. The theoretical modeling of the shell and the finite element formulation in the moving coordinate system are presented in Section 2, while the conditions for instability and the value of the critical velocity for uniform shells are described in Section 3. Section 4 extends the analysis of Section 3 to the case of stiffened shells and introduces the transfer matrix formulation. Also in Section 4, the behavior of stiffened shells is presented for different configurations of the stiffening rings. Section 5 summarizes the main results of this work and gives some recommendation for future investigations.

2. Finite element model of shells with moving load

2.1. Basic assumptions and kinematic relations

The shell model is formulated according to Donnel-Mushtari theory for thin shells [15]. The theory assumes the shell radial displacement W to be constant across the thickness and equal to the displacement of the mid-surface of the cylinder w:

$$W(x, r, t) = w(x, t). \tag{1}$$

In addition, here only axi-symmetric radial vibrations are analyzed and therefore the displacement in Eq. (1) is considered independent from the circumferential angle θ (see Fig. 1).

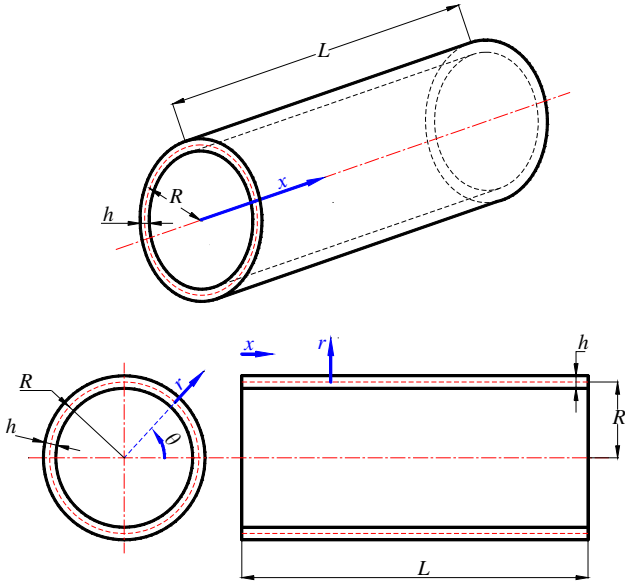

Fig. 1. Cylindrical shell and coordinate system.

The strain components are related to the axial and radial displacements of the mid-surface of the shell through the following expressions [15]:

$$\varepsilon_x = r\frac{\partial^2 w}{\partial x^2}, \quad \varepsilon_\vartheta = \frac{w}{R}, \quad \gamma_{x\vartheta} = 0. \tag{2}$$

2.2. Distributed parameter model

The equations governing the dynamics of the shell can be obtained by applying Hamilton's principle:

$$\delta \int_{t_1}^{t_2} (U - T + W_e)\,\mathrm{d}t = 0, \tag{3}$$

where $\delta(.)$ denotes the first variation, 't' denotes time and t_1, t_2 define the integration time limits. In Eq. (3), U and T are, respectively, the strain and kinetic energy of the shell, while W_e denotes the work of the external forces.

According to the current assumptions, the shell strain and kinetic energies can be defined as

$$U = \pi \int_0^L \int_{-h/2}^{h/2} (\sigma_x \varepsilon_x + \sigma_\vartheta \varepsilon_\vartheta)(R + r)\,\mathrm{d}r\,\mathrm{d}x. \tag{4}$$

and

$$T = \pi \cdot \rho \int_0^L \dot{w}^2 hR\,\mathrm{d}x, \tag{5}$$

where h, L and R denote, respectively, the thickness, the length and the radius of the shell as shown in Fig. 1, and ρ is the density of the shell material.

The external load is a radial impulse traveling at constant speed v along the shell length. The corresponding work can be therefore expressed as

$$W_e = \int_0^L F_0 \cdot \delta(x - v \cdot t) w(x, t)\,\mathrm{d}t, \tag{6}$$

where F_0 is the magnitude of the applied load.

The resulting equation of motion describing the radial axisymmetric vibration of the shell is

$$D\frac{\partial^4 w}{\partial x^4}+\frac{K}{R^2}w+\rho h\frac{\partial^2 w}{\partial t^2}=F_0\cdot\delta(x-vt), \tag{7}$$

where $K=Eh/(1-\nu^2)$ is the membrane stiffness and $D=Eh^3/(12(1-\nu^2))$ is the bending stiffness of the shell, E being the Young's modulus of the material.

Eq. (7) can be conveniently rewritten in a coordinate system ξ moving with the load such that

$$\xi=x-vt, \tag{8}$$

with the radial response of the shell, under the load, given by

$$\bar{w}(\xi)=w(x-vt). \tag{9}$$

Imposing the new coordinate system, Eq. (7) becomes:

$$D\frac{\partial^4 \bar{w}}{\partial \xi^4}+\rho h\cdot v^2\frac{\partial^2 \bar{w}}{\partial \xi^2}-2\rho h\cdot v^2\frac{\partial^2 \bar{w}}{\partial \xi\partial t}+\rho h\frac{\partial^2 \bar{w}}{\partial t^2}+\frac{K}{R^2}\bar{w}=F_0\cdot\delta(\xi). \tag{10}$$

If the amplitude and the velocity of the applied load are invariant with time, and if the steady-state response of the shell is considered, then all the partial derivatives with respect to time in Eq. (10) can be set to zero.

Eq. (10) thus simplifies to

$$D\frac{\mathrm{d}^4 \bar{w}}{\mathrm{d}\xi^4}+\rho h\cdot v^2\frac{\mathrm{d}^2 \bar{w}}{\mathrm{d}\xi^2}+\frac{K}{R^2}\bar{w}=F_0\cdot\delta(\xi). \tag{11}$$

Under steady-state conditions and a coordinate system moving with the load, the dynamic response of the shell can be determined by solving the static deformation problem expressed by Eq. (11), whose solution provides the radial displacement of the shell for a concentrated load at $\xi=0$.

The solution of Eq. (10) is written in the form

$$\bar{w}(\xi)=A_1\mathrm{e}^{-k_1\xi}+A_2\mathrm{e}^{-k_2\xi}+A_3\mathrm{e}^{k_1\xi}+A_4\mathrm{e}^{k_2\xi}, \tag{12}$$

where and A_1, A_2, A_3, A_4, are the constants to be determined by imposing the boundary conditions, while k_1 and k_2 are obtained from the characteristic equation associated with Eq. (11) and are, respectively, given by:

$$k_1^2=-\frac{\rho h v^2}{2D}+\frac{1}{2D}\sqrt{(\rho h v^2)^2-4\frac{K}{R^2}D}$$

and

$$k_2^2=-\frac{\rho h v^2}{2D}-\frac{1}{2D}\sqrt{(\rho h v^2)^2-4\frac{K}{R^2}D}. \tag{13}$$

Eq. (12) provides the radial vibration for a shell with uniform geometrical and material properties.

2.3. Finite element formulation in the moving coordinate system

For a shell with thickness varying along the length as shown in Fig. 2, the radial deformations can be determined by discretizing the shell into uniform finite elements. Two nodal points bound the considered one-dimensional shell elements, each node has two degrees of freedom to describe the radial displacement and slope. The nodal deflection vector $\{\Delta\}$ of each element is given by

$$\{\Delta\}=\left\{\bar{w}_i,\bar{w}_i',\bar{w}_j,\bar{w}_j'\right\}^{\mathrm{T}}, \tag{14}$$

where the subscripts 'i' and 'j' denote, respectively, the left and right node of the element while the primes indicate the spatial derivative with respect to ξ.

As the radial displacement within each element is described by Eq. (12), then the constants A_1, A_2, A_3, and A_4 can be related to the element nodal deflection vector by imposing the displacements at the boundaries.

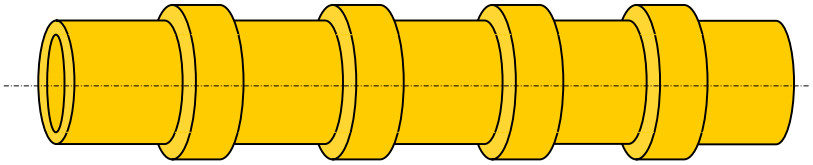

Fig. 2. Stiffened shell.

Accordingly, the displacement field in one element can be written as

$$\bar{w}(\xi) = [N(\xi)]\{\Delta\}, \tag{15}$$

where $[N(\xi)]$ is the matrix of the interpolation functions for the considered shell element, which describes the displacement of any point along the shell in terms of the nodal deflection vector. The interpolation functions are obtained from the solution of Eq. (11) and therefore, for a uniform shell, they reproduce the exact displacements.

The internal generalized forces at the nodal locations can be obtained as

$$\begin{Bmatrix} S_i \\ M_i \\ S_j \\ M_j \end{Bmatrix} = \begin{Bmatrix} -D \cdot \bar{w}_i''' \\ D \cdot \bar{w}_i'' \\ D \cdot \bar{w}_j''' \\ -D \cdot \bar{w}_j'' \end{Bmatrix}. \tag{16}$$

Substituting Eq. (15) in Eq. (16), yields a relation between the generalized loads at the nodes and the nodal displacement vector:

$$\begin{Bmatrix} S_i \\ M_i \\ S_j \\ M_j \end{Bmatrix} = \begin{bmatrix} -D \cdot N'''(\xi_i) \\ D \cdot N''(\xi_i) \\ D \cdot N'''(\xi_j) \\ -D \cdot N''(\xi_j) \end{bmatrix} \{\Delta\}, \tag{17}$$

where ξ_i and ξ_j are, respectively, the coordinates of the left and right node of the element in the moving coordinate system. Eq. (17) can be rewritten as

$$\{F\} = [K]\{\Delta\}, \tag{18}$$

where $[K]$ represents the stiffness matrix of the shell element and $\{F\}$ is the nodal load vector. Assembly of the different elements by using classical finite element techniques gives the equilibrium equation of the considered shell in the moving coordinate system. The resulting equation provides the radial vibration of a shell subjected to a load moving axially along the shell at a constant speed.

Solution of Eq. (11) gives the corresponding interpolation functions for a given shell dimensions and material as well as for a given load velocity. These functions are then used to form the stiffness matrix, as given by Eq. (18). The deflection vector $\{\Delta\}$ can then be computed depending on the location of the load.

3. Response and critical velocity of uniform shells

A uniform aluminum shell with inner and outer diameters of 0.01375 m (0.55″) and 0.0156 m (0.625″) is first considered. The shell is loaded by a moving radial force of unit amplitude. The shell response is evaluated directly by using Eq. (12) and by imposing free–free boundary conditions. A major result that can be highlighted from this analysis is the existence of a critical velocity, where the amplitude of the steady-state response becomes infinite [10]. This behavior is displayed in Fig. 3, where the maximum amplitude of the response for the considered shell is plotted at different load velocities. The plot clearly demonstrate the

dependence of the response on the load velocity and highlights the presence of a peak amplitude at a critical velocity v of 1425 m/s.

Previous studies indicated that such a critical velocity corresponds to load velocity that is equal to the minimum velocity at which waves can propagate along the shell [10]. The radial response for a uniform shell as expressed by Eq. (12), results in fact from the superposition of four waves with wavenumbers $\pm k_1$ and $\pm k_2$ propagating along the moving coordinate ξ. It is well known that waves are free to propagate when the real part of the associated wavenumbers is equal to zero. From Eq. (13), it can be easily verified that the real part of the wavenumbers becomes zero when $v > v_{cr}$, with v_{cr} given by:

$$v_{cr} = \left(\frac{4KD}{\rho^2 h^2}\right)^{1/4}. \tag{19}$$

The real parts of k_1 and k_2 are plotted, in Fig. 4, against the load velocity v normalized with respect to v_{cr}. The plot indicates that for any velocity above v_{cr}, the real part of the wavenumbers is always equal to zero. Accordingly, for $v > v_{cr}$ the perturbation introduced by the moving load is free to propagate along the shell length in the moving coordinate system. Hence, for a uniform shell the load velocity can either belong to a

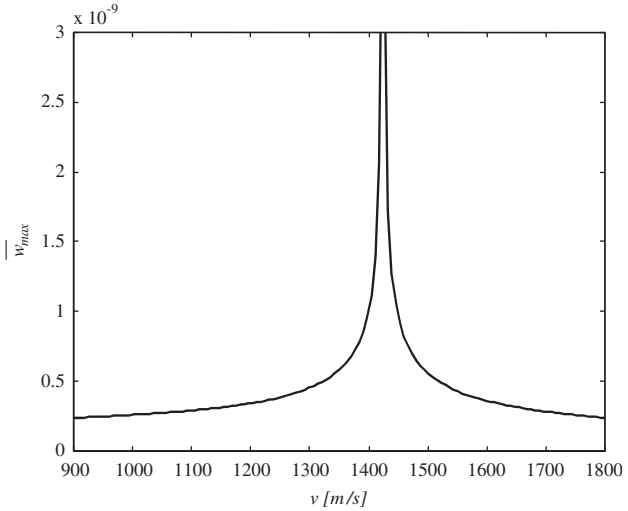

Fig. 3. Maximum shell response versus load velocity.

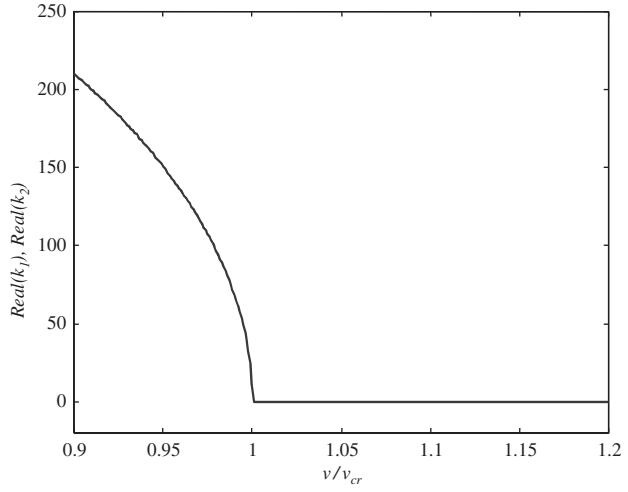

Fig. 4. Real part of the wavenumbers versus load velocity.

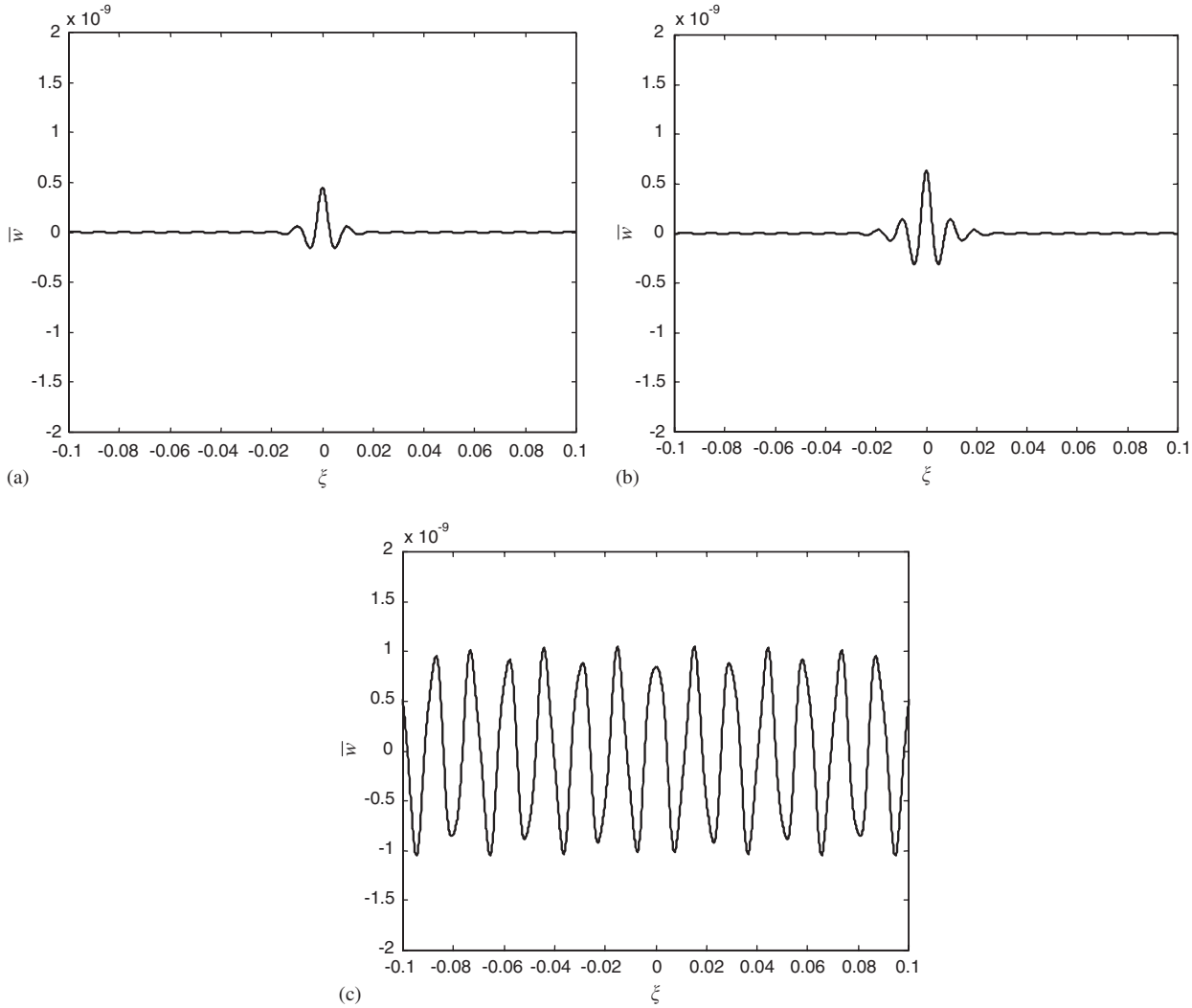

Fig. 5. Response of a uniform shell to a load moving at various velocities: (a) $v/v_{cr} = 0.8$, (b) $v/v_{cr} = 0.9$, (c) $v/v_{cr} = 1.2$.

sub-critical range, if $v < v_{cr}$, or to a critical range if $v > v_{cr}$. The shell response for velocities in the sub-critical and critical ranges is shown in Fig. 5. In the sub-critical range, the displayed examples emphasize that increasing the load velocity increases also the amplitude of the shell response. In the critical range, i.e. for $v > v_{cr}$, the radial deformation propagates away from the load. The transition between sub-critical and critical conditions is visualized in Fig. 6, which summarizes the concepts discussed above.

The results presented in this section indicate that the steady-state behavior of a shell, under moving load, can be conveniently studied as a wave propagation phenomenon. Also, the stability conditions can be identified by evaluating the parameters governing the dynamics of wave propagation along the moving coordinate system.

4. Response and critical velocities for stiffened shells

4.1. Overview

The results obtained in the previous section are extended to the analysis of stiffened shells. The steady-state response of stiffened shells is predicted by means of the finite element formulation presented in Section 2. The

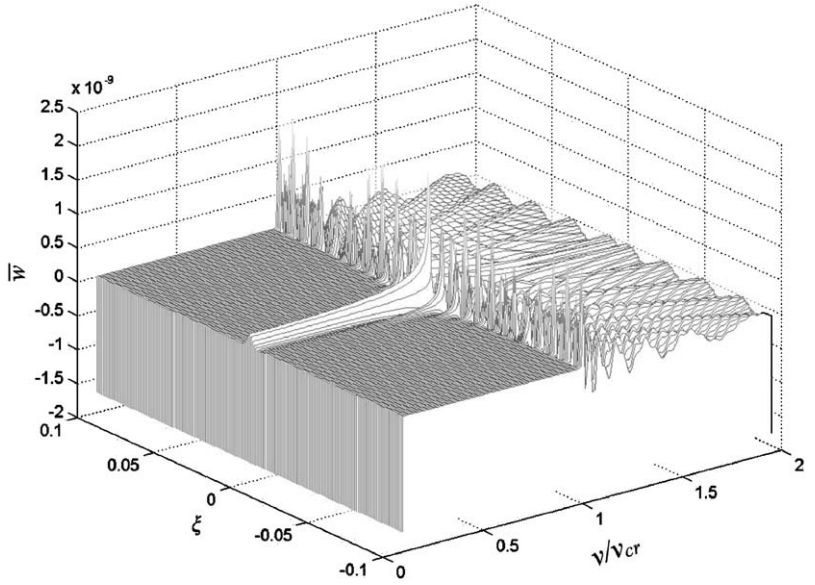

Fig. 6. Transition between sub-critical and critical conditions for a uniform shell.

stiffeners are modeled as uniform elements of higher radial thickness that are periodically placed along the shell (Fig. 2). Studying the dynamics of wave propagation in stiffened shells yields the stability conditions of these shells when subjected to loads moving at constant velocity. The wave propagation in the considered shell structure can be conveniently analyzed through a transfer matrix formulation, which can be easily derived from the FEM of Section 2. Emphasis is placed here on assessing the effect of the axial spacing of the stiffeners and of their thickness on the response and the critical velocity of the shell.

4.2. Shell geometry and material properties

An aluminum shell with inner and outer diameters of 0.01375 m (0.55″) and 0.0156 m (0.625″) is considered. The stiffening rings have an axial length of 0.004 m (0.1575″). The stiffener axial length = 0.004 m. The moving load is a radial force of unit amplitude.

4.3. Transfer matrix formulation

The stiffened shell shown in Fig. 2 can be studied as an assembly of a number of identical stiffened elements joined together in an identical manner. Each stiffened element can be modeled by two shell elements of uniform thickness as shown in Fig. 7. For each element, the nodal displacements are related to the nodal loads by the stiffness matrix introduced in Eq. (18), which can be rewritten as

$$\begin{bmatrix} K_{LL} & K_{LR} \\ K_{RL} & K_{RR} \end{bmatrix} \begin{Bmatrix} \Delta_L \\ \Delta_R \end{Bmatrix} = \begin{Bmatrix} F_L \\ F_R \end{Bmatrix}, \tag{20}$$

where K_{ij} and F_i are sub-matrices of $[K]$ and $\{F\}$. Also, the subscripts L and R denote the left and right nodes of the considered uniform element.

Eq. (20) can be rearranged to relate generalized forces and displacements at the right and left of the element:

$$\begin{Bmatrix} \Delta_R \\ F_R \end{Bmatrix} = \begin{bmatrix} -K_{LR}^{-1}K_{LL} & K_{LR}^{-1} \\ K_{RR}K_{LR}^{-1}K_{LL} - K_{RL} & -K_{RR}K_{LR}^{-1} \end{bmatrix} \begin{Bmatrix} \Delta_L \\ F_L \end{Bmatrix}. \tag{21}$$

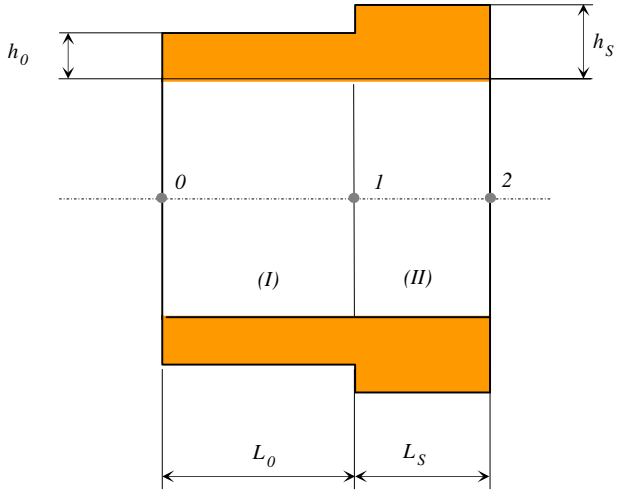

Fig. 7. Stiffened shell element.

In compact form:

$$\{Y_R\} = [T]\{Y_L\}, \tag{22}$$

where $\{Y_i\} = \{\Delta_i, F_i\}^{\mathrm{T}}$ is the state vector at ith end of the shell element, and $[T]$ is element transfer matrix.

The transfer matrix formulation described by Eq. (22) can be utilized to relate the state vector at node '0' to the state vector at node '2' of the stiffened element shown in Fig. 7. In particular, the state vectors at the right end of the uniform elements I and II can be expressed as

$$\{Y_1\} = \left[T^{(\mathrm{I})}\right]\{Y_0\}$$

and

$$\{Y_2\} = \left[T^{(\mathrm{II})}\right]\{Y_1\}, \tag{23}$$

where $\left[T^{(\mathrm{I})}\right]$ and $\left[T^{(\mathrm{II})}\right]$ are the transfer matrices of elements I and II, respectively.

Imposing the continuity of displacements as well as the equilibrium at the elements interface yields:

$$\{Y_1\} = \left[T^{(\mathrm{II})}\right] \cdot \left[T^{(\mathrm{I})}\right]\{Y_0\},$$

or

$$\{Y_2\} = [T_S]\{Y_0\}, \tag{24}$$

where $[T_S]$ is transfer matrix for the stiffened element. The transfer matrix $[T_S]$ is characterized by two frequency-dependent eigenvalues:

$$\lambda_1 = \mathrm{e}^{\mu_1}, \quad \lambda_2 = \mathrm{e}^{\mu_2}$$

and

$$\lambda_3 = \mathrm{e}^{-\mu_1}, \quad \lambda_4 = \mathrm{e}^{-\mu_2}, \tag{25}$$

where the parameters μ_1 and μ_2 are called propagation constants. The eigenvalues of $[T_S]$ are obtained by solving the following eigenvalue problem:

$$[T_S]\{Y_0\} = \lambda\{Y_0\}. \tag{26}$$

Combining Eqs. (24) and (26), gives:

$$\{Y_2\} = \lambda\{Y_0\} = \mathrm{e}^{\mu}\{Y_0\}, \tag{27}$$

which indicates that the state vectors at the beginning and at the end of the stiffened element can be related through the eigenvalues of the transfer matrix. The eigenvalues and the corresponding propagation constants determine the nature of the wave dynamics in the considered structure. The real part of μ represents the decay of the amplitude of a wave propagating from one end of the stiffened element to the other. Wave propagation is therefore possible for the values of the load velocity that correspond to the real part of the propagation constants equal to zero. Hence, analyzing the value of the propagation constants for different load velocities identifies the critical conditions for moving loads in stiffened shells composed of a sequence of elements as the one depicted in Fig. 7.

4.4. Critical velocities

The influence of the stiffeners on the critical velocities is investigated for the shell whose properties are listed in Table 1. A comparison between uniform, or un-stiffened, and stiffened shells is carried out by analyzing the propagation constants obtained from the eigenvalues of the transfer matrix of the element shown in Fig. 7. The analysis is performed for different stiffener thickness h_s and different length L_0 of the un-stiffened portion of the element. Note that the value of L_0 defines the spacing between two consecutive stiffeners.

The real parts of the propagation constants corresponding to different configurations are plotted against the load velocity in Fig. 8. Fig. 8a is obtained for fixed spacing and varying thickness h_s, the case of uniform shell is obtained by setting $h_s = h_0$. For the case of uniform shell, the real parts of the propagation constants are equal to zero for any value of velocity above 1425 m/s. This behavior indicates that waves propagate along the shell for loads moving at velocities above this value, which matches the value of the critical velocity calculated from Eq. (19). Increasing the thickness h_s increases the critical velocity and therefore expands the sub-critical range. Furthermore, additional zones above the first critical velocity where waves do not propagate are generated. Hence, stiffening the shell increases the critical velocity and generates an alternating pattern of non-critical (white areas) and critical regions (shaded areas). The width of the non-critical range can be modified by changing the thickness of the stiffeners (Fig. 8a) and/or their spacing (Fig. 8b). Complete representations of the critical regions for varying thickness and stiffeners spacing are presented, respectively, in Fig. 9a and b. In these figures, the shaded areas define instability zones. Fig. 9a is obtained for ratios h_s/h_0 varying between 1, which corresponds to the case of uniform shell, to 2. The map confirms that for $h_s/h_0 = 1$ every value of velocity above 1425 m/s is critical. It also shows that increasing the thickness expands the sub-critical range and generates a pattern of alternating non-critical and critical zones, the latter being represented as shaded areas. Similar behavior can be observed if the stiffeners' spacing is varied as shown in Fig. 9b. The map indicates that reducing the spacing generally shifts all the critical areas towards higher velocities. Also, it suggests that increasing the ratio L_0/L_s, make the first critical velocity converge to the value for uniform shells (1425 m/s).

4.5. Steady-state response

The results presented in the previous section can be confirmed by evaluating the shell steady-state response. The response of a shell provided by eight stiffened elements with $h_s/h_0 = 1.2$ and $L_s/L_0 = 10$ is compared with

Table 1
Material properties and geometry of the shell

Young's modulus	$E = 71$ GPa
Poisson's ratio	$v = 0.3$
Density	$\rho = 2700\,\mathrm{Kg/m^3}$
Shell length	$L = 55.88$ cm (22″
Shell internal diameter	$D_I = 1.4$ cm (0.55″
Shell external diameter	$D_0 = 1.59$ cm (0.625″)
Shell thickness	$h_0 = 0.953$ mm (0.375″)
Stiffeners axial length	$L_s = 4$ mm (0.1575″)

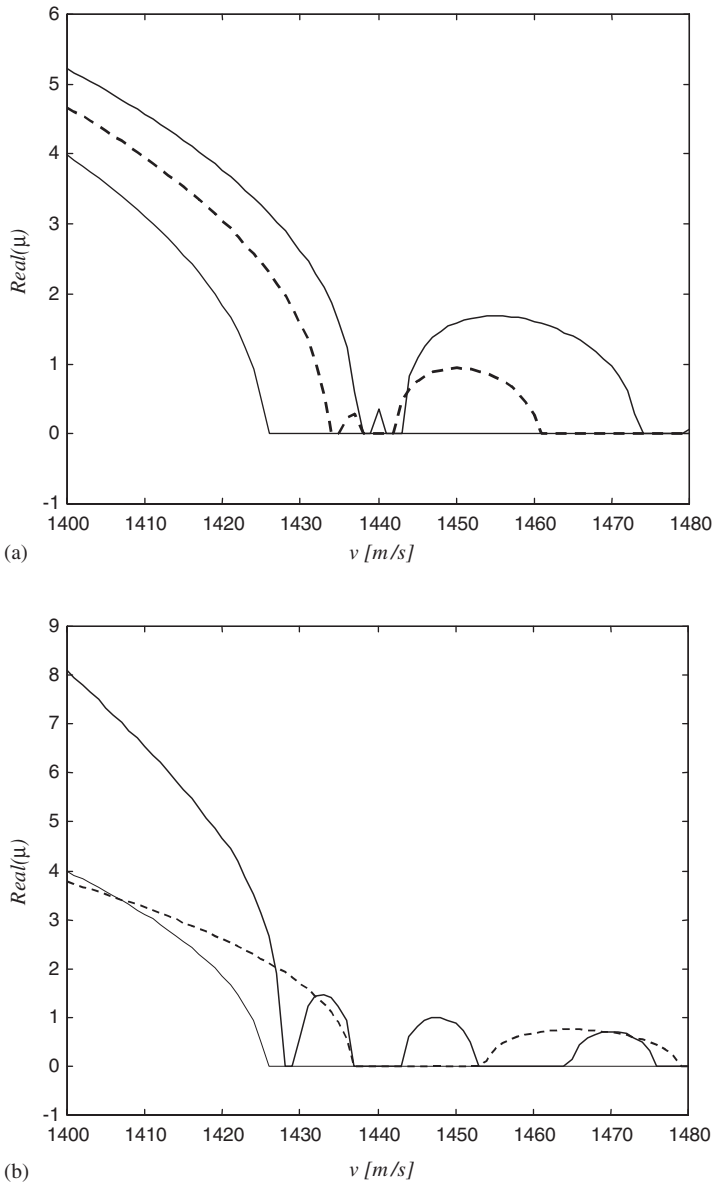

Fig. 8. Propagation constants for varying thickness (a) and spacing (b) of one stiffener. (a) —— Uniform shell, - - - - $h_s/h_0 = 1.2$, $L_0/L_s = 10$, —— $h_s/h_0 = 1.5$, $L_0/L_s = 10$; (b) —— uniform shell, - - - - $h_s/h_0 = 1.2$, $L_0/L_s = 7.5$, —— $h_s/h_0 = 1.2$, $L_0/L_s = 20$.

that of a uniform shell. The comparison is carried out for different load velocities. Fig. 10a is obtained for a sub-critical load velocity of 1410 m/s, which in both shells corresponds to a radial deformation concentrated around the location of the load. For a velocity of 1430 m/s (Fig. 10b), the radial response is free to propagate in the uniform shell, but it is still localized in the stiffened shell, in accordance to the predictions formulated by means of the propagation constants analysis. A similar behavior can be observed for a load velocity of 1450 m/s, which, for the considered stiffened shell, belongs to the second non-critical region (see Figs. 8 and 9).

The location and width of the critical regions as determined from the propagation constants may be also verified by evaluating the response at the shell end, when the load is located at the beginning of the shell. In a sub-critical range, the excitation remains localized near the load, while for critical velocities the perturbation

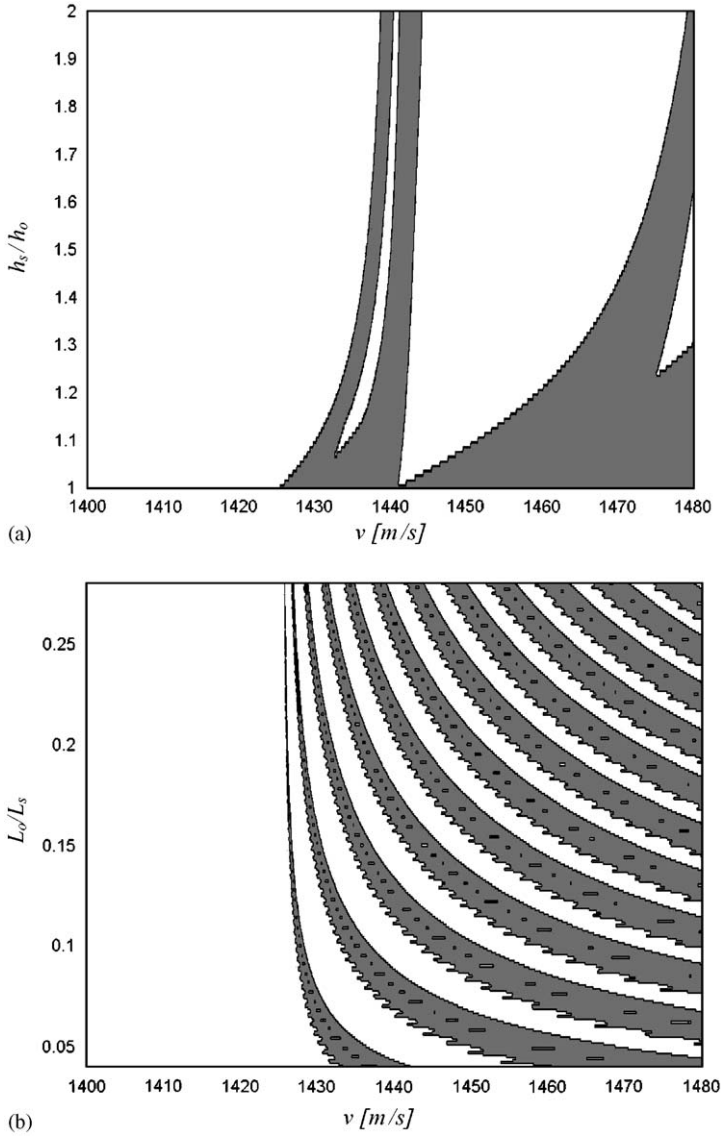

Fig. 9. Regions of critical velocity for varying stiffeners' thickness for $L_0/L_s = 10$ (a) and spacing for $h_s/h_0 = 1.2$ (b).

propagates along the shell length. Accordingly, the amplitude of the response far from the applied load is small for non-critical velocities, while it becomes relevant within critical regions. This concept is demonstrated in Fig. 11, where the responses of uniform and stiffened shells are compared. The plots highlight the values of the velocity where the excitation propagates to the shell end, which correspond to the critical velocity ranges predicted by the analysis of the propagation constants (Fig. 8).

5. Conclusions

The dynamic response of axi-symmetric shells to moving loads is analyzed. Periodic placement of stiffening rings along the shell stiffens the shell and improves their dynamic stability characteristics. The shell response is determined through a finite element model, formulated in a coordinate system moving with the load. The model utilizes shape functions obtained from the steady-state solution of the equation of motion for a uniform

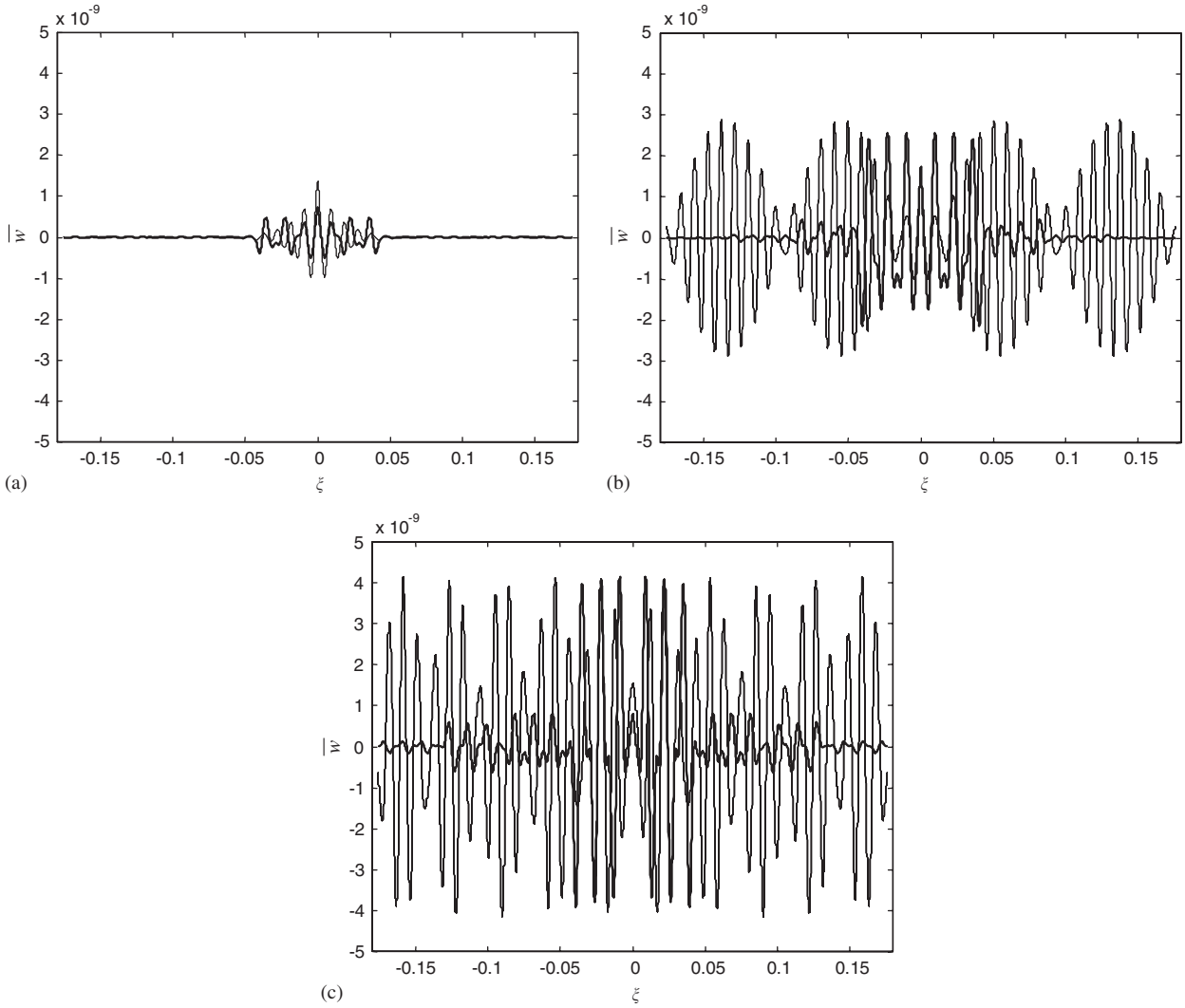

Fig. 10. Shell response for $v = 1410\,\mathrm{m/s}$ (a), $v = 1430\,\mathrm{m/s}$ (b) and $v = 1450\,\mathrm{m/s}$ (c) (—— uniform shell, —— $h_s/h_0 = 1.2$, $L_0/L_s = 10$).

shell. This formulation allows for analyzing the shell stability using wave propagation and attenuation criteria. The critical velocity is identified as the minimum velocity allowing propagation of the applied perturbation. For a stiffened shell, such conditions can be conveniently identified through a transfer matrix formulation, which is obtained from the developed finite element model. The transfer matrix formulation provides a flexible tool for determining the critical velocities for shells with stiffeners of different configurations. The proposed approach is used to assess the effect of stiffeners' thickness and spacing on the stability regions. The presented results indicate that stiffening the shell generally improves its dynamic behavior, by extending the velocity range of stability and by generating additional non-critical velocity ranges. The steady-state response of stiffened shells, evaluated for various load velocities, confirms the predictions obtained from the analysis of the transfer function and demonstrates the effectiveness of the proposed approach.

The presented study should be extended to include the effect of moving masses on the shell's stability and to predict non-axi-symmetric deformation. Furthermore, the presented numerical results should be validated experimentally. Experiments are now being carried out using the University of Maryland Air Gun which is capable of firing 20 moving masses/min at speeds reaching 2000 m/s.

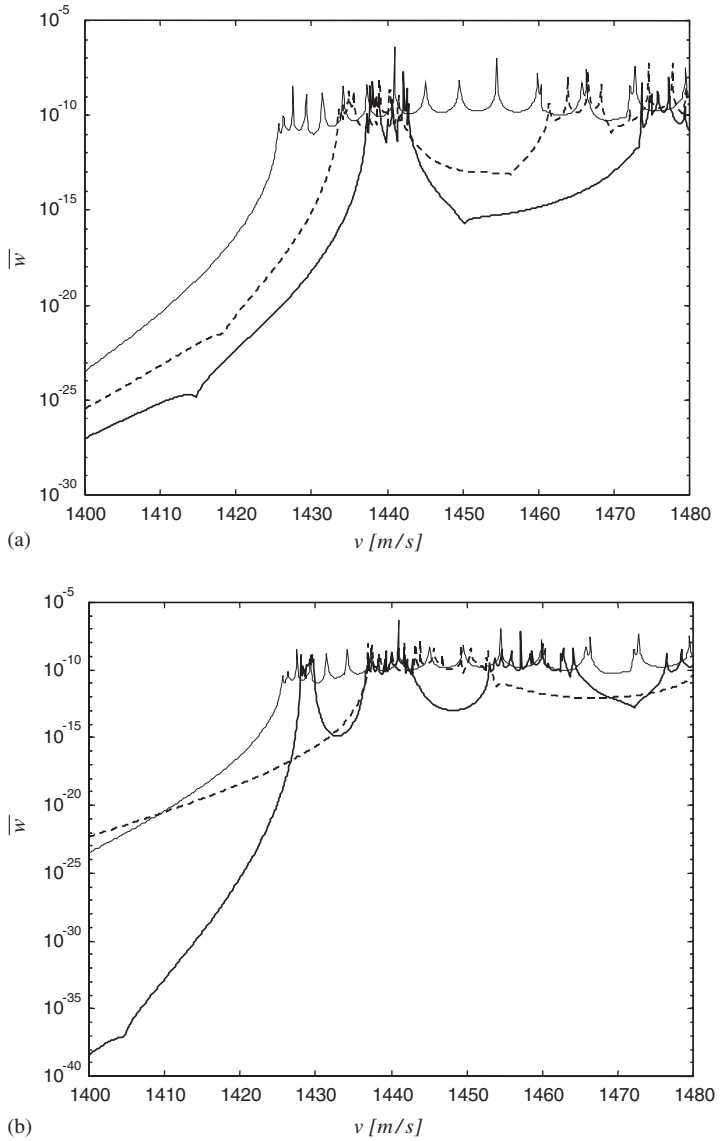

Fig. 11. Shell response for varying thickness (a) and spacing (b) of stiffeners. (a) —— Uniform shell, - - - -. $h_s/h_0 = 1.2$, $L_0/L_s = 10$, —— $h_s/h_0 = 1.5$, $L_0/L_s = 10$; (b) —— uniform shell, - - - - $h_s/h_0 = 1.2$, $L_0/L_s = 7.5$, —— $h_s/h_0 = 1.2$, $L_0/L_s = 20$.

Acknowledgements

This work is funded by The US Army Research Office (Grant Number DAAD199910200). Special thanks are due to Dr. Gary Anderson, the technical monitor, for his invaluable technical inputs.

References

[1] L. Fryba, *Vibration of Solids and Structures Under Moving Loads*, Noordhoff International, Groningen, The Netherlands, 1977.
[2] M. Abu-Hilal, M. Mohsen, Vibration of beams with general boundary conditions due to a moving harmonic load, *Journal of Sound and Vibration* 232 (4) (2000) 703–717.
[3] Y.-H. Lin, M.W. Trethewey, Finite element analysis of elastic beams subjected to moving dynamic loads, *Journal of Sound and Vibration* 136 (4) (1990) 323–342.

[4] H.D. Nelson, R.A. Conover, Dynamic stability of a beam carrying moving masses, *ASME Journal of Applied Mechanics* 38 (1971) 1003–1006.
[5] C.R. Steele, The finite beam with a moving load, *ASME Journal of Applied Mechanics* 34 (1) (1967) 111.
[6] C.R. Steele, The Timoshenko beam with a moving load, *ASME Journal of Applied Mechanics* 40 (1973) 481–488.
[7] V.V. Bolotin, *The Dynamic Stability of Elastic Systems*, Holden Day Inc., San Francisco, 1964.
[8] G.A. Benedetti, Dynamic stability of a beam loaded by a sequence of moving mass particles, *ASME Journal of Applied Mechanics* 41 (1974) 1069–1071.
[9] R. Katz, C.W. Lee, A.G. Ulsoy, R.A. Scott, Dynamic stability and response of a beam subject to a deflection dependent moving load, *ASME Journal of Vibration, Acoustics, Stress and Reliability in Design* 109 (1987) 361–365.
[10] J.R. Kenney, Steady-state vibration of beam on elastic foundation for moving load, *ASME Journal of Applied Mechanics* 21 (4) (1954) 359–364.
[11] D. F. Finlayson, Characterization of the dynamic strain excitation force in gun tubes, *Ninth Symposium of Gun Dynamics*, SAVIAC, Baltimore, MD, November 2000, pp. 12.1–12.16.
[12] O.J. Aldareirhem, A. Baz, Dynamic stability of periodic stepped beams under moving loads, *Journal of Sound and Vibration* 50 (5) (2002) 835–848.
[13] C.S. Hsu, Impulsive parametric excitation: theory, *ASME Journal of Applied Mechanics* 39 (1972) 551–558.
[14] C.S. Hsu, W.-H. Cheng, Application of the theory of impulsive parametric excitation and new treatments of general parametric excitation problems, *ASME Journal of Applied Mechanics* 40 (1973) 78–86.
[15] W. Soedel, *Vibration of Shells and Plates*, Marcel Dekker, New York, 1993.